MATTER: International Journal of Science and Technology
ISSN 2454-5880

Piloto et al., 2017

Volume 3 Issue 3, pp. 13-23

Date of Publication: 15th November 2017

DOI-https://dx.doi.org/10.20319/mijst.2017.32.1323

This paper can be cited as: Piloto, P., Khetata, M., & Gavilán, A. (2017). Fire Performance of Non-Loadbearing Light Steel Framing Walls – Numerical and Simple Calculation Methods. MATTER: International Journal of Science and Technology, 3(3), 13-23.

FIRE PERFORMANCE OF NON-LOADBEARING LIGHT STEEL FRAMING WALLS – NUMERICAL AND SIMPLE CALCULATION METHODS

Paulo A. G. Piloto
LAETA-INEGI, Polytechnic Institute of Bragança, Bragança, Portugal
ppiloto@ipb.pt

Mohamed S. Khetata
Sci. & Tech. Park Brigantia-EcoPark, Bragança, Portugal
khetatamohamedseddik@gmail.com

Ana B. R. Gavilán
Dep. of Mech. Engineering, University of Salamanca, Zamora, Spain
aramos@usal.es

Abstract

Light steel frame and prefabricated panels are widely used in non-loadbearing walls, with direct application to steel framed buildings. Such panels consist of steel sections (studs and tracks) with gypsum plasterboard layers attached to the flanges on the outside and use insulation material in the cavities. The fire resistance is usually provided by one or more layers of panels and by the insulation material. This investigation evaluates the thermal behaviour of the unexposed surface and of the nodal internal layers, using numerical simulations and a simple calculation method, assuming that heat flow is almost one-dimensional. The fire resistance is compared for both models using a cross section of the wall with one and two gypsum layers. The

insulation criterion is the only one used for the calculation of the fire resistance, based on the calculation of the average and maximum temperature of the unexposed surface above the initial average temperature. Good approach was achieved by the simple calculation model, when optimum effective width is assumed for the model.

Keywords

LSF Walls, Fire Resistance, Numerical Simulation, Simple Calculation Method

1. Introduction

Light steel sections and prefabricated panels are widely used in non-load-bearing walls, with direct application to timber, concrete and steel framed buildings. There is a wide range of application buildings, such as multi storey offices, educational buildings, health buildings, residential buildings and other type of public buildings. The fire protection is usually provided by one or more layers of fire protection materials. Members which meet fire resistance standards are the result of the proper combination of certain materials and members. The thin steel sections must be covered with a sheathing to prevent them from being damaged by fire. Gypsum plates and rockwool insulation have been approved as fire protection materials and can be combined with steel to build fire resistance walls.

To prevent fire propagation into adjacent compartments, partition walls must meet the requirements for fire resistance, preventing the propagation of fire (integrity -E) and limiting the temperature of the unexposed surface (insulation -I) in the fire compartment. The fire resistance (insulation criterion) of this construction element depends on the temperature evolution in the unexposed surface. The performance of the building products is regulated by the European standard EN13501-2 (CEN, 2009), which specifies the fire classification of construction products and building elements, using data from fire resistance test. The European standard used to determine experimentally the fire resistance for non-loadbearing elements - Part 1 is dedicated to non-loadbearing walls (CEN, 2015). These tests are usually expensive and numerical methods can be used to estimate this fire resistance, in particular the insulation-I criterion.

The installation of an insulation material eventually reduces heat convection, radiation and conduction in the internal cavity. This material protection may also be important to increase the integrity-E performance criterion, due to the common failure of the panel exposed to fire. If the insulation material is not required to achieve the insulation-I performance criteria, is normally required to increase the acoustic efficiency.

Each component of the non-loadbearing, such as the panels, the insulation, the lightweight steel structure and its location determines the category of the whole member's fire resistance category. The spacing of plates, the thickness and the number of coating layers, the thermal properties of the materials as well as the width of the insulation material are decisive for the classification of the member.

Two distinct numerical methods were considered in this investigation. The two-dimensional finite element model uses conventional incremental and nonlinear transient thermal analysis (ANSYS). The one dimensional strip model uses incremental and nonlinear transient solution and was developed for comparison, assuming that heat flows across the section by well-defined patterns. This last method is simple to use, less time consuming and was already validated with experiments (Shahbazian, A., & Wang, Y. C, 2013).

2. Non-Load Bearing Walls

The non-loadbearing walls under analysis are made of a light steel frame structure (studs and tracks) separated by 190 mm each stud. Two different layers of gypsum with 12.5 mm thickness each and rockwool insulation material protect this light steel frame. Figure 1 represents the front view and a cross section for the case 1C (one layer) and case 1D (two layers). The geometry of this wall is representative of the full-scale wall. The assembly uses vertical members (studs) made of steel GD280 using the profile C90x43x15x1.5 and horizontal members (tracks) made of steel GD280 using the profile U93x43x1.5. The reference code gives the dimensions of the web, flange, lip and thickness of steel.

One side of the wall is going to be submitted to fire and the other side is assumed to remain at room temperature. The boundary conditions are defined in accordance to EN1991-1-2 (CEN, 2002), assuming heat transfer by radiation (emissivity of fire $\varepsilon_f = 1$) and convection (convection coefficient $\alpha_c = 25 \left[W / m^2 K \right]$) in the exposed side and heat transfer by convection (convection coefficient $\alpha_c = 9 \left[W / m^2 K \right]$ to include the radiation component) in the unexposed side. The temperature in the exposed side follows the standard ISO834 (ISO, 1999).

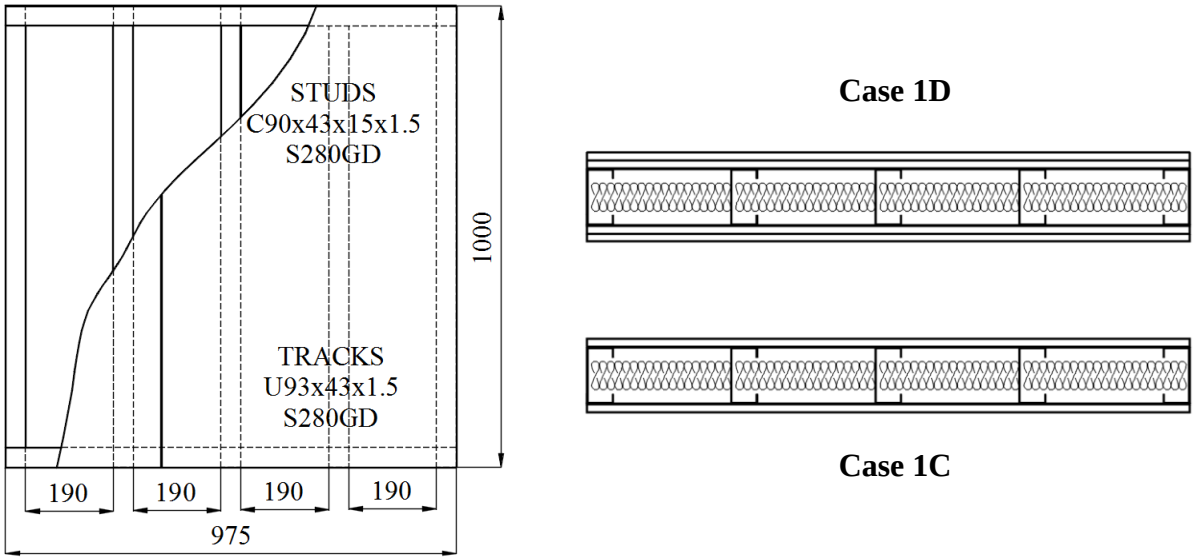

Figure 1: *Non-Loadbearing Wall (Dimensions in mm)*

3. Material Properties

The thermal properties are decisive to simulate the performance of the non-loadbearing wall. The thermal properties are temperature dependent for all the materials involved.

Steel presents typical evolution for the specific heat (C_{ps}) with a maximum value that account to the allotropic transformation, thermal conductivity (λ_s) and specific mass (ρ_s), see Figure 2, (CEN, 2005). The thermal properties of Gypsum X type considered in this investigation were determined by experiments (Sultan, 1996), using Differential Scanning Calorimeter (DSC) for the specific heat (C_{pg}), Thermal Conductivity Meter for conductivity (λ_g) and a vacuum conditioning chamber for the specific mass (ρ_g), see Figure 2. The thermal properties of the Rockwool depends on the fabrication process. During the production process, the fibres are pressed to achieve different densities, being the heaviest ones produced as boards and the lightest as mats. The specific mass of this material (ρ_i) was considered equal to 120 kg/m³, being the specific heat (C_{pi}) and thermal conductivity (λ_i) temperature dependent, see Figure 2. The fibre itself starts melting around 1000 ºC (Steinar Lundberg, 1997).

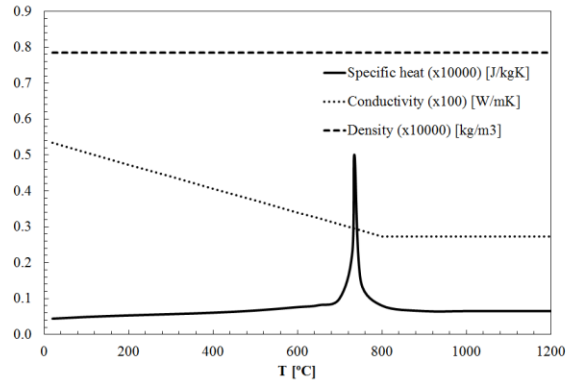

a) Steel

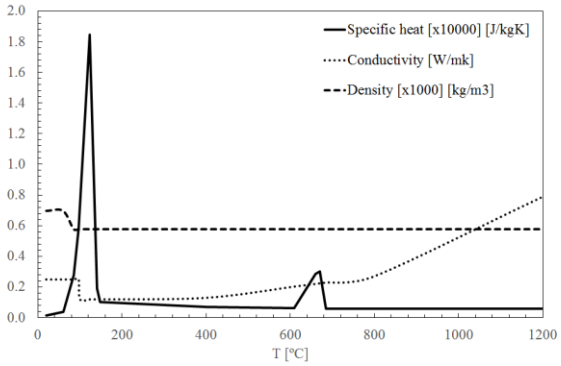

b) Gypsum

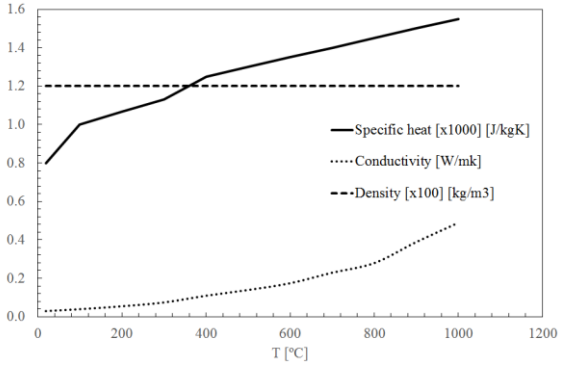

c) Rockwool

Figure 2: *Thermal Properties of Steel, Gypsum and Rockwool*

4. Numerical Model

The finite element model was used to define part of the cross section of the non-loadbearing wall. The model uses PLANE 55 finite element, which has a 2-D thermal conduction capability. The element has four nodes with a single degree of freedom (temperature at each node). This element has linear interpolating functions and uses four points to developed full integration gauss method over quadrilaterals. The mesh was defined based on a convergence test. The solution used an incremental and iterative method to solve the nonlinear transient thermal problem. The convergence was based on the calculation of the internal heat flow, with a minimum reference value of 1E-6 and a tolerance value of 0.001. The time step was define to be 60 s with a minimum of 5 s to achieve convergence. Figure 3 represents the mesh for case 1C and 1D, the nodal temperatures for the critical time, based on the criterion (Insulation –I) used to define the fire resistance.

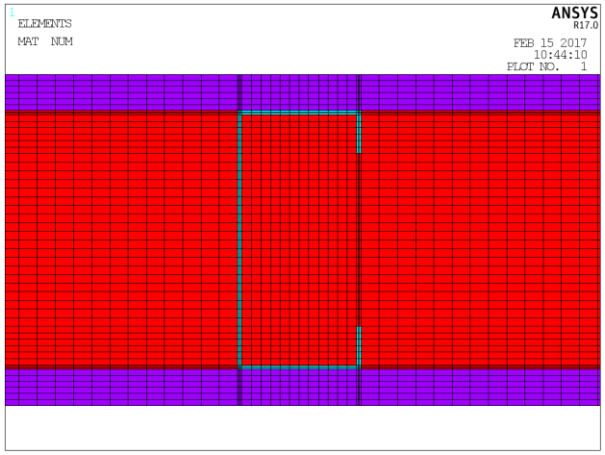

a) Mesh for Case 1C

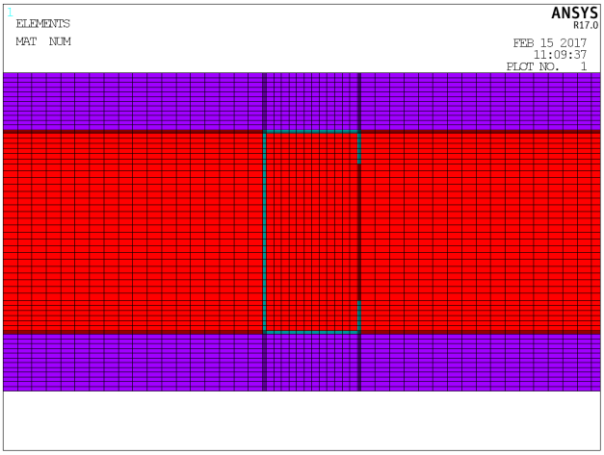

b) Mesh for Case 1D

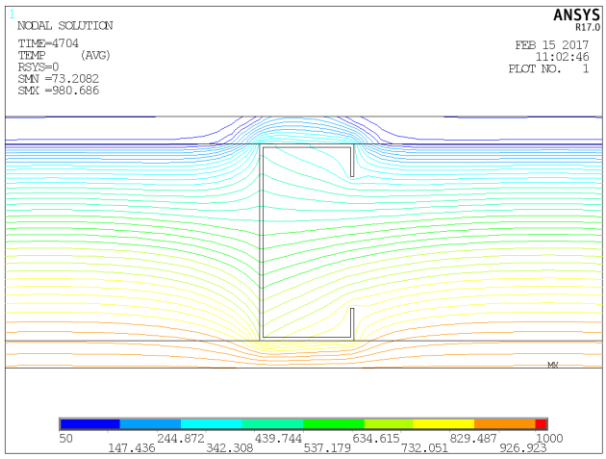

c) Temperature (critical time 78.4 min) - Case 1C

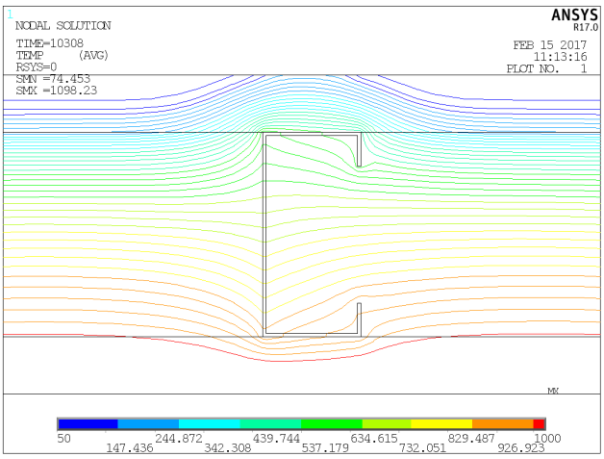

c) Temperature (critical time 171.8 min) - Case 1D

Figure 3: *Mesh and results from 2D analysis (ANSYS)*

The lip-flange corner of the stud presents higher temperature when compared to the flange-web corner of the same profile, for both cases on the exposed side. The temperature of the lip-flange corner is smaller than the temperature of the flange-web corner, for both cases on the unexposed side of the wall. This behaviour may be justified by the higher heat flux expected on the web of the stud, due to smaller heat conduction resistance. The numerical model was already validated against the experimental results of other investigation (Prakash Kolarkar, 2010).

The temperature field analysis is of great importance for the selection of the effective width (w_e) to be considered in the one-dimensional heat transfer analysis.

5. Simple Calculation Model

The simple calculation model is based on one-dimensional analysis, considering the finite difference method and the lumped thermal method.

This model uses 14 layers or regions with width equal to the effective width (w_e) and 14 nodes to define temperature in the cross section that includes the steel stud, see Figure 4. The geometry (thickness equals TG/4) and material properties of layers 2, 3, 4, 11, 12, 13 are similar. Layer 1 and 14 have similar geometry and material properties (thickness equals TG/8). Layer 5 and 10 are similar and have mixed materials (gypsum, rockwool and steel). Layer 6 and 9 have similar geometry and material and layers 7 and 8 also.

This model was submitted to fire in one side (convection and radiation boundary conditions) and to room temperature in the unexposed side (convection boundary condition). The flow pattern is also depicted in Figure 4, representing the heat resistance possibility to heat conduction through the cross section.

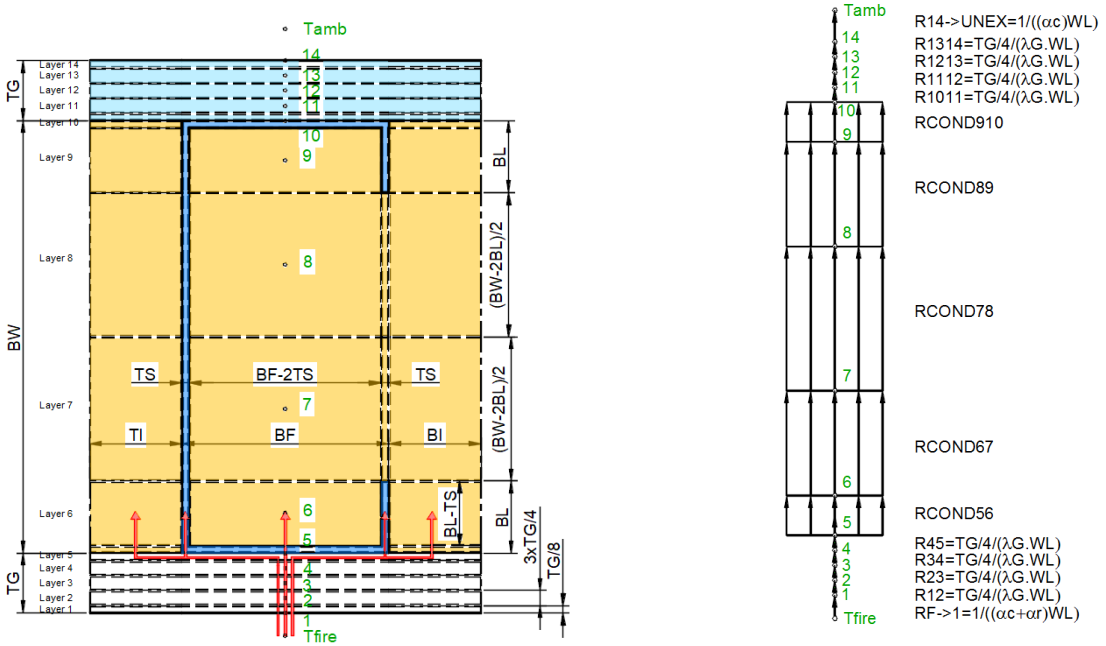

a) Layers and nodes for heat transfer b) Heat flow pattern

Figure 4: *Layer model and flow pattern for one dimensional heat transfer*

This model is based on the heat balance of each layer, taking into consideration the amount of heat flux entering the layer and the amount of heat flux leaving the layer. The difference between these values corresponds to the amount of heat required to increase the

temperature of the layer from the previous time step T_i^{t-1} to the current one T_i , see Equations 1-14. Equation 1 was linearized to solve a system of linear equations.

$$\alpha(T_{fire}-T_1)W_e+\varepsilon_f\varepsilon_m\sigma(T_{fire}+T_1)(T_{fire}^2+T_1^2)(T_{fire}-T_1)W_e-\lambda_G/(TG/4)(T_1-T_2)W_e=\rho_G\,Cp_G\,(TG/8)(T_1-T_1^{t-1})/\Delta t\,W_e \quad (1)$$

$$\lambda_G/(TG/4)(T_1-T_2)W_e-\lambda_G/(TG/4)(T_2-T_3)W_e=\rho_G\,Cp_G\,(TG/4)(T_2-T_2^{t-1})/\Delta t\,W_e \quad (2)$$

$$\lambda_G/(TG/4)(T_2-T_3)W_e-\lambda_G/(TG/4)(T_3-T_4)W_e=\rho_G\,Cp_G\,(TG/4)(T_3-T_3^{t-1})/\Delta t\,W_e \quad (3)$$

$$\lambda_G/(TG/4)(T_3-T_4)W_e-\lambda_G/(TG/4)(T_4-T_5)W_e=\rho_G\,Cp_G\,(TG/4)(T_4-T_4^{t-1})/\Delta t\,W_e \quad (4)$$

$$\lambda_G/(TG/4)(T_4-T_5)W_e-(T_5-T_6)/R_{COND56}=(T_5-T_5^{t-1})/RCAP5 \quad (5)$$

$$(T_5-T_6)/R_{COND56}-(T_6-T_7)/R_{COND67}=(T_6-T_6^{t-1})/RCAP6 \quad (6)$$

$$(T_6-T_7)/R_{COND67}-(T_7-T_8)/R_{COND78}=(T_7-T_7^{t-1})/RCAP7 \quad (7)$$

$$(T_7-T_8)/R_{COND78}-(T_8-T_9)/R_{COND89}=(T_8-T_8^{t-1})/RCAP8 \quad (8)$$

$$(T_8-T_9)/R_{COND89}-(T_9-T_{10})/R_{COND910}=(T_9-T_9^{t-1})/RCAP9 \quad (9)$$

$$(T_9-T_{10})/R_{COND910}-\lambda_G/(TG/4)(T_{10}-T_{11})W_e=(T_{10}-T_{10}^{t-1})/RCAP10 \quad (10)$$

$$\lambda_G/(TG/4)(T_{10}-T_{11})W_e-\lambda_G/(TG/4)(T_{11}-T_{12})W_e=\rho_G\,Cp_G\,(TG/4)(T_{11}-T_{11}^{t-1})/\Delta t\,W_e \quad (11)$$

$$\lambda_G/(TG/4)(T_{11}-T_{12})W_e-\lambda_G/(TG/4)(T_{12}-T_{13})W_e=\rho_G\,Cp_G\,(TG/4)(T_{12}-T_{12}^{t-1})/\Delta t\,W_e \quad (12)$$

$$\lambda_G/(TG/4)(T_{12}-T_{13})W_e-\lambda_G/(TG/4)(T_{13}-T_{14})W_e=\rho_G\,Cp_G\,(TG/4)(T_{13}-T_{13}^{t-1})/\Delta t\,W_e \quad (13)$$

$$\lambda_G/(TG/4)(T_{13}-T_{14})W_e-\alpha_c(T_{14}-T_{amb})W_e=\rho_G\,Cp_G\,(TG/8)(T_{14}-T_{14}^{t-1})/\Delta t\,W_e \quad (14)$$

The parameter $R_{COND\,i\,j}$ represents the resistance to heat flow by conduction expected from node i to node j due to parallel heat flow pattern and should be calculated as the equivalent resistance. This parameter should be evaluated at the average temperature of both nodes i and j. The parameter R_{CAPi} represents the inverse of the thermal capacitance of layer i and should be evaluated at the temperature of layer i. The thermal conductivity of gypsum λ_G should be evaluated at the average temperature of the nodes involved, while the density ρ_G and

the specific heat C_{PG} should be evaluated at the temperature level of the corresponding layer (Shahbazian, A., & Wang, Y. C, 2013). The time step was define to be 1 s and validate the stability criterion (Sultan, M. A., 1996).

6. Comparison of Results

The fire resistance of the non-loadbearing wall depends on the calculation of the unexposed temperature of the wall. This temperature is not uniform and depends on the quantity of steel included in this type of non-loadbearing wall. The performance criteria used for this construction element accounts for the calculation of the average temperature T_{AVE} and maximum temperature T_{MAX} (CEN, 2012). The maximum temperature is achieved on the back of the steel stud. The average temperature was calculated at the gypsum surface, taking into consideration 17 modal values, representative of the unexposed side.

The performance level used to define insulation shall be the average temperature rise on the unexposed surface limited to 140 °C above the initial average temperature, or, with the maximum temperature rise at any point limited to 180 °C above the initial average temperature (CEN, 2012).

The one-dimensional model takes into to consideration the existence of the steel stud, reason why the results are close to the T_{MAX} temperature, see Figure 5.

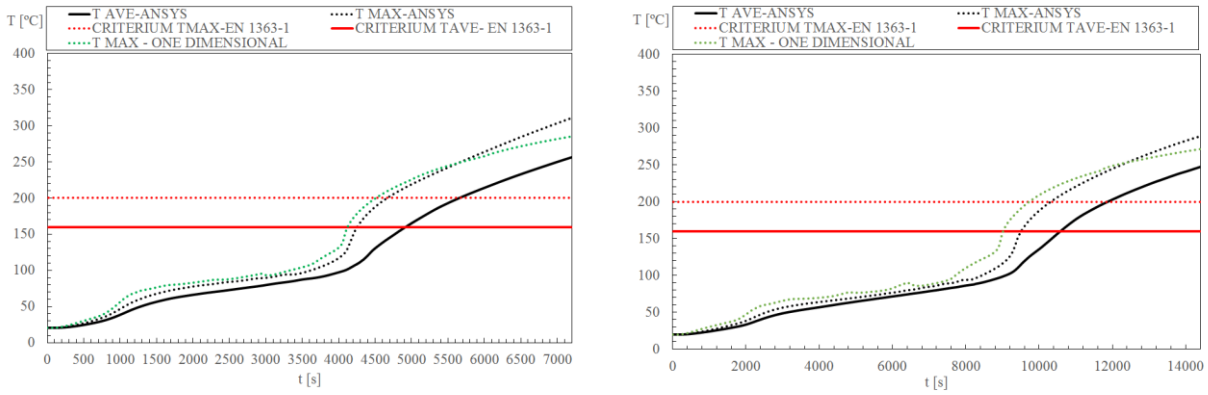

a) Results for Case 1C

b) Results for Case 1D

Figure 5: *Temperature results using both solution methods*

The fire resistance is compared in Table 1, in completed minutes for which the specimen continues to maintain its separating function during the simulation without developing critical

temperatures on its unexposed surface. The results calculated by the one-dimensional model are between 3.8 % and 5.2 % smaller than the ones obtained by two-dimensional model.

Table 1: *Fire Resistance*

Solution method	Case 1C	Case 1D
Ansys 2D (1)	78 [min]	171 [min]
One-dimensional (2)	75 [min]	162 [min]
Relative difference |(2)-(1)|/(1)	3.8%	5.2%
Class of fire resistance	I 60	I 120

7. Conclusions

The fire performance of non-loadbearing LSF wall was determined by two different solution methods with good agreement. Comparison was developed for two different cases (case 1C with one gypsum panel and case 1D with two gypsum panels). The fire resistance increased 120% with the increase of 100% the value of the thickness of the panel.

The numerical simulation of the two-dimensional cross section allows the temperature calculation in all materials in general and the assessment of the unexposed surface temperature in particular. This method requires the definition of geometric model and meshing procedures, which may be time consuming.

The one-dimensional method is an approaching solution that considers uniform temperature in each layer and one-dimensional flow pattern through the thickness of the wall, involving all the materials crossed by the heat flow. This method requires the definition of the dimensions for the steel stud and mainly the effective width of the model used to consider the flow pattern. This method can be used at a preliminary design stage, is easy to be used and avoid cost effective experimental tests. The effective width of the model should be well predicted to achieve good results in comparison to the numerical simulation results.

This research takes part of an extended experimental investigation, used to determine the behaviour of LSF walls, in particular the fire resistance of new composite materials and also to validate different numerical models (solid and fluid thermal analysis).

References

CEN - European Committee for Standardization (2002). EN 1991-1-2 - Eurocode 1: Actions on structures - Part 1-2: General actions - Actions on structures exposed to fire (pp. 59). Brussels, November.

CEN - European Committee for Standardization (2005). EN 1993-1-2 - Eurocode 3: Design of steel structures - Part 1-2: General rules - Structural fire design (pp. 78). Brussels, April.

CEN- European Committee for Standardization (2009), EN 13501-2 - Fire classification of construction products and building elements - Part 2: Classification using data from fire resistance tests, excluding ventilation services; (pp. 79). Brussels, September.

CEN- European committee for standardization (2012). EN 1363-1: Fire resistance tests - Part 1: General Requirements (pp. 52). Brussels: July.

CEN- European Committee for Standardization (2015). EN 1364-1 - Fire resistance tests for non-loadbearing elements. Part 1: Walls; (pp. 66). Brussels, July.

ISO - Technical Committee ISO/TC 92. (1999). ISO 834-1. Fire-resistance tests - Elements of building construction – Part 1: general requirements (pp. 25). Switzerland, September.

Prakash Nagaraj Kolarkar, "Structural and thermal performance of cold-formed steel stud wall systems under fire conditions", PhD thesis at Queensland University of Technology, pp: (412), September 2010.

Shahbazian, A., & Wang, Y. C. (2013). A simplified approach for calculating temperatures in axially loaded cold-formed thin-walled steel studs in wall panel assemblies exposed to fire from one side. Thin-Walled Structures, 64, (pp: 60-72). https://doi.org/10.1016/j.tws.2012.12.005

Steinar Lundberg (1997). Material Aspects of Fire Design. TALAT Lectures 2502 (training in Aluminium Application Technologies, Leonardo da Vinci project TAS/WP (pp. 21). EAA - European Aluminium Association.

Sultan, M. A. (1996). A model for predicting neat transfer through non-insulated unloaded steel stud gypsum board wall assemblies exposed to fire. Fire Technology, 32(3); (pp: 239-259). https://doi.org/10.1007/BF01040217